Author Manuscript

Author Manuscript

Author Manuscript

Author Manuscript

HHS Public Access

Author manuscript

Biomech Model Mechanobiol. Author manuscript; available in PMC 2018 December 13.

Published in final edited form as:

Biomech Model Mechanobiol. 2018 February ; 17(1): 87–101. doi:10.1007/s10237-017-0946-y.

Mechanobiological model of arterial growth and remodeling

Maziyar Keshavarzian[1], **Clark A. Meyer**[1], and **Heather N. Hayenga**[#1]

[1]Department of Biomedical Engineering, The University of Texas at Dallas, 800 W. Campbell Road, Richardson, TX 75080, USA

[#] These authors contributed equally to this work.

Abstract

A coupled agent-based model (ABM) and finite element analysis (FEA) computational framework is developed to study the interplay of bio-chemo-mechanical factors in blood vessels and their role in maintaining homeostasis. The agent-based model implements the power of REPAST Simphony libraries and adapts its environment for biological simulations. Coupling a continuum-level model (FEA) to a cellular-level model (ABM) has enabled this computational framework to capture the response of blood vessels to increased or decreased levels of growth factors, proteases and other signaling molecules (on the micro scale) as well as altered blood pressure. Performance of the model is assessed by simulating porcine left anterior descending artery under normotensive conditions and transient increases in blood pressure and by analyzing sensitivity of the model to variations in the rule parameters of the ABM. These simulations proved that the model is stable under normotensive conditions and can recover from transient increases in blood pressure. Sensitivity studies revealed that the model is most sensitive to variations in the concentration of growth factors that affect cellular proliferation and regulate extracellular matrix composition (mainly collagen).

Keywords

Agent-based modeling; Finite element analysis; Coronary artery; Multiscale modeling

1 Introduction

The coordinated ability of blood vessels to maintain homeostasis and adapt to mechanobiological alterations in their environment requires an orchestra of events that stretch across various biological scales. At the cellular level, cells are known to respond to the presence of various growth factors, signaling molecules and changes in mechanical stress by proliferating, participating in programmed death, or modulating the composition of the extracellular matrix (ECM) (Intengan and Schiffrin 2001; Korshunov et al. 2007; Schiffrin 2012). These events are triggered within minutes to hours of a change in their environment

Conflict of interest

The authors declare that they have no conflict of interest.

Electronic supplementary material The online version of this article (doi:10.1007/s10237-017-0946-y) contains supplementary material, which is available to authorized users.

Author Manuscript Author Manuscript Author Manuscript Author Manuscript

and can continue for days to weeks. Within weeks to months, these biological responses can collectively change the structure and mechanical properties of a blood vessel, thereby affecting its state of stress (Intengan and Schiffrin 2001; Fridez et al. 2002; Hayashi and Naiki 2009). This iterative process results in continual and spatiotemporally dependent growth and remodeling. Despite the wealth of information available in the literature regarding various mechanisms involved in maintaining arterial homeostasis and adaptation, a holistic point of view that spatiotemporally correlates the net of biological events to underlying mechanics is still lacking (Hayenga et al. 2013). The challenge we face is not necessarily due to a lack of knowledge about individual mechanisms involved, but rather due to our inability to compare, contrast and integrate the ocean of information available in the literature into a comprehensive scenario that can describe various aspects of compensatory arterial growth and remodeling. Computational models can act as a valuable tool for conceptualizing the complex web of mechanobiological processes involved in arterial adaptation (Hayenga et al. 2011; Cockrell et al. 2015). Modeling vascular adaptation requires a model that can account for the interaction and regulation of cells and their ECM content as well as calculate and respond to changes in stress and strain levels within the artery wall of a blood vessel. Agent-based modeling (ABM) has been used to study cellular interactions. This flexible technique enables simulation of complex biological systems at the cellular level with high spatial and temporal resolution. In these models, agents(i.e., cells in this case) are individual autonomous objects that behave and interact according to a set of predefined rules. The resulting interaction of these agents determines the overall response of system. Although ABMs are known to provide insightful information regarding emergent behaviors in biological systems (Boyle et al. 2010; Thorne et al. 2011), existing ABMs either overlook the role of mechanical stimuli in regulation of homeostasis or take simplistic approaches toward the calculation of stress and strain (Thorne et al. 2011). This limitation is mainly due to an inherent inability of ABMs to easily calculate the stress and strain in the time varying, non-homogeneous and complex geometry of the artery. To address this issue, researchers have suggested coupling ABMs with continuum-level models. We have previously coupled ABM with constrained mixture models (Hayenga et al. 2013). However, these models were incapable of capturing non-axisymmetric spatial variations in mechanical properties, a shortcoming that can be addressed by coupling ABM and FEA models. Coupled ABM and FEA models have been used to study intimal hyperplasia in a tissue engineered vessel (Zahedmanesh and Lally 2012) and stent restenosis (Boyle et al. 2013; Zahedmanesh et al. 2014). Zahedmanesh et al. (2014) modeled response of smooth muscle cells (SMCs) to placement of a stent, defined production of matrix metalloproteinase-2 (MMP-2) by SMCs as a function of mechanical damage and used a constant doubling time for proliferation of synthetic SMCs. Boyle et al. (2013) used a combination of an injury model, inflammation model and SMC model to simulate stent restenosis.

To achieve the ultimate goal of using the ABM to capture emergent behaviors within the arterial wall, it is crucial to include the role of various soluble factors (e.g., growth factors and proteases) and their interactions. Herein, we present a coupled ABM-FEA computational framework that allows for fast and reliable simulation of vascular adaptation by coupling cellular production of growth factors and proteases to changes in stress and strain. This ABM includes three major cell types within the artery and accounts for cellular

Author Manuscript Author Manuscript Author Manuscript Author Manuscript

production of three different proteases, MMP-1, 2 and 9, two growth factors, platelet-derived growth factor-AB (PDGF-AB) and tissue growth factor-beta (TGF-rbeta), and two endogenous paracrines, nitric oxide (NO) and endothelin-1 (ET-1). Performance of the model was assessed under normotensive conditions and under transient increases in blood pressures. Also, sensitivity of model to variations of ABM parameters is assessed by performing a 1D sensitivity analysis. This model can be used as a tool to study emergent aspects of vascular remodeling, predicting arterial responses under pathological conditions, or as a quantitative measure for comparing results reported by various researchers.

2 Materials and methods

A computational framework that allows fast and reliable coupled ABM-FEA simulation of blood vessels was developed in Java™. REPAST Simphony libraries (North et al. 2013) were used as the base code for the ABM and the commercially available FE package ANSYS (ANSYS Inc., Canonsburg, PA) for FEA simulations. A 3D model of porcine left anterior descending artery (LAD) was implemented, and we conducted stability checks and parameter sensitivity analysis for select parameters. The model is constructed based on histological data available from a porcine model of hypertension that provided information regarding initial cell density and amount of structurally significant ECM proteins as well as geometry of the LAD (Hayenga et al. 2012), and details are provided in Table 2 in supplementary documents. Cell size is chosen based on information provided by Chamley-Campbell et al. (1979) for SMCs and adventitial fibroblasts (AFs) and Garipcan et al. (2011) for endothelial cells (ECs); cell volumes are reported in supplemental Table 3.

2.1 Agent-based model

The ABM expands upon a 2D model of mouse aorta (Thorne et al. 2011) developed in Netlogo (Wilensky and Evanston 1999). The ABM module implements the REPAST Simphony libraries (North et al. 2013) and adapts this environment for 3D lattice-based biological simulations. Two super classes of agents were defined in this model: *patch* and *cell*. *Patches* are stationary agents of dimension 25μm 25μm × 25μm that contain space filling ECM, *cells*, as well as various chemokines and growth factors secreted by *cells*. Each lattice site can be occupied by one agent of type *patch* and multiple agents of type *cell*. These two super classes were supplemented with a set of methods that define their general behavior, such as the ability to identify and update their type, identify neighbors of a specific class, manage their contents and diffuse various cytokines and growth factors. Each subclass, for instance, different types of *cells*, is then provided with specific rules that define its behavior in response to changes in their *patch* environment. These rules include cell-type-specific relationships governing production of various growth factors and proteases, deposition and degradation of collagen, elastin and gelatin, as well as proliferation and apoptosis in the presence of various factors. A forward in time, centered in space, discretization algorithm is implemented in the ABM code to solve Fickian diffusion equations.

The *patch* super class consists of four subclasses: *intimal*, *medial*, *adventitial* and *boundary*. Each of *intimal*, *medial* and *adventitial patches* is associated with a subclass of *cells* (ECs,

Author Manuscript Author Manuscript Author Manuscript Author Manuscript

SMCs and AFs). *Patch* type is initially assigned based on information provided by user regarding geometrical features of the artery during model initialization step and is updated based on the cell types occupying the *patch* during simulation. For instance, SMCs can move into and out of an *adventitial patch*; however, *patch* type will only update from *adventitial* to *medial* when the last fibroblast moves out of the *patch*. Each *patch* has a constant volume and manages its contents so that the occupied volume never surpasses the nominal volume. This management is performed by calculating the ratio of occupied volume to nominal volume (V_{ratio}) for all *patches*, identifying *patches* with a ratio greater than one, choosing a content (SMC, EC, AF) randomly, making a list of neighbors that have a lower ratio in comparison with the over occupied *patch* and moving the extra content (i.e., cells) to those *patches*. In generating the list of neighbors, priority is with *patches* associated with chosen content, two scenarios are possible if no such *patch* is found. If chosen content is in a *patch* which is not associated with it, another content is picked and procedure is repeated from beginning. Otherwise, the search is gradually extended to (i) *patches* of the same type, (ii) *patch* types that are part of the artery (*intimal*, *medial* and *adventitial*) and (iii) finally all patch types (including *boundary*). For instance, an extra SMC in a *medial patch* can move to an *adventitial patch* only if it cannot find any neighboring *medial patch* with a lower V_{ratio}. Upon moving to an *adventitial patch*, the SMC prefers to move back to a *medial patch*, but if no adjacent *medial patch* with a lower V_{ratio} is found it will stay in the *adventitial patch*.

The model is constructed based on information provided by the user regarding geometrical features of the artery, composition of each layer, volume of various cell types and lattice size; this information can be provided either by using the graphical user interface (GUI) or a text file (Fig. 1). The cubic lattice is then populated with patches that contain appropriate number of cells and amount of ECM. The simulated blood vessel was assumed to consist of three layers—intima, media and adventitia, and each of these layers was represented by a *patch* type. The three cell types included in the model were ECs, SMCs and AFs. The rules for each cell type are found in Table 1. To reduce computational cost, the model represents cells of some types in multiples. That is, each *cell* representing an EC actually contains four ECs and each *cell* representing a SMC contains two SMCs, but an AF is represented as one *cell*. Considering that mechanical stimuli and alterations in blood pressure are key players in regulation of homeostasis in blood vessels, the ABM was designed to take into account these effects by automatically creating a FE model of the artery using ANSYS Parametric Design Language (APDL) and reading in the calculated stress and strain values for each patch from the FE model via text files. A time step (or tick in ABM terminology) of 6h was chosen for the ABM based on studies by Thorne et al. (2011).

2.1.1 Rule development—Each rule of the ABM describes a certain aspect of an agents behavior, and rule derivation is the conversion of the data gleaned from literature into mathematical equations and systematic language. As this model aims to eventually predict arterial adaptation in response to alterations in blood pressure, rules included in the model were focused on regulation of ECM and production of key vasoactive paracrines, growth factors and matrix metalloproteases involved in this process. Collagen type I, elastin and gelatin comprise the ECM, and elastin turnover was assumed to be insignificant under

Author Manuscript Author Manuscript Author Manuscript Author Manuscript

normal conditions (given its long half-life of 40 years (Lefevre and Rucker 1980)). Table 1 presents a full list of rules and macromolecules incorporated into the model.

2.1.2 Rule scoring—Reliability of ABM predictions depends on the quality and credibility of the information used to generate the rules. Discrepancies within a rule can arise, as the information was obtained from various sources with experiments performed according to different protocols, equipment and cell types. Therefore, it is necessary to assess the quality of each rule diligently. To address this issue, a rule scoring method suggested by Thorne et al. (2011) was used. In short, a weighted average score was calculated based on metrics assessing literature consensus or number of peer-reviewed articles in agreement with the rule, physiological methods or similarity to in vivo conditions, similarity metric (same cell type, species and organ system to that being simulated) and data type that checks if the data were extrapolated or obtained from direct measurements. The scoring procedure was repeated by at least two researchers. Each rule is scored on a scale of 0 to 10, with 10 being the highest. For instance, in literature consensus metric a rule will receive a score of 10 if 7 or more papers confirm its results and a score of 0 if the results are not confirmed by other researchers. More details are given in Table 1 in supplementary documents. In order to improve the quality of predictions, rules that received an average composite score below 5 were reexamined and re-derived if possible.

2.2 Finite element analysis

The finite element model is created automatically using an ANSYS Parametric Design Language (APDL) script that is generated by an interaction module within the ABM. This interaction module is run every 5 time steps (every 30 h); it collects information on each *patch*'s position, composition and blood pressure from the ABM in order to update a preexisting template for APDL script accordingly. The APDL script constructs the geometry, generates a mesh using cubic SOLID186 elements, assigns pointwise material properties to each element, applies boundary conditions and load, runs the solver in batch mode and writes desired the outputs of maximum principal stress and strain to a text file. The interaction module then assigns the outputs to corresponding *patches*. The entire handshaking procedure takes 4min to complete for a normotensive simulation.

Arterial tissue was modeled as an isotropic inhomogeneous material with incompressible neo-Hookean hyper-elastic properties. A content-based strain energy density function, inspired by models presented by Zulliger et al. (2004) and Karšaj and Humphrey (2012), was developed using the USERMAT feature of ANSYS. The material model receives mass fractions and initial shear modulus of four groups of contents to calculate strain energy density at each integration point. These groups include collagen, elastin, cells and gelatin. The material constants were obtained by reviewing literature for collagen (Lu et al. 2004), elastin (Lu et al. 2004; Karšaj et al. 2010), cells (Engler et al. 2004; Qiu et al. 2010; Stroka and Aranda-Espinoza 2011) and gelatin (Norris and McGraw 1964; Lou 1999; Yakimets et al. 2005) (Table 2). Equation 1 shows strain energy density function implemented in the USERMAT of ANSYS in which φ_i is the mass fraction of content i, c_i is material constant and I_1 is first invariant of the right Cauchy Green tensor. Although it might be ideal for each element to have its own unique material defined in ANSYS, this is not possible due to

Author Manuscript Author Manuscript Author Manuscript Author Manuscript

technical limitations on number of materials within ANSYS. Therefore, a table containing possible permutations of mass fractions for various contents (steps of 5%) was defined in the ABM. The ABM chooses the material that is closest to the combination of mass fractions for each *patch*, and flags it to be passed to FEA.

$$W = \sum_{i=1}^{4} \phi_i \cdot w_i = \sum_{i=1}^{4} \phi_i \cdot \frac{c_i}{2}(I_1 - 1) \quad (1)$$

FEA simulations were performed under normotensive conditions (mean arterial pressure=13.3 kPa, based on (Hayenga et al. 2012) with an axial prestretch of 10% (Guo et al. 2012) and a preconditioned conjugate gradient (PCG) solver. To validate FEA predictions, as a first step, circumferential stress was compared to values obtained from analytical models (homogenous thick-walled cylinder) and subsequently inner radius (under normotensive conditions) was compared to experimental values reported by Broek et al. (2011).

2.3 Homeostatic stability and sensitivity analysis

While this model aims to capture emergent behaviors during arterial adaptation, under healthy normotensive conditions there should not be any significant change in matrix contents nor cell proliferation or apoptosis rates. Therefore, it is crucial to ensure that the model is stable under homeostatic conditions and under transient changes in blood pressure and that the sensitivity of outputs to variations of various parameters implemented in each rule is assessed. First, parametric refinement was performed to ensure that the model is stable under homeostatic conditions. Subsequently, the ability of the model to recover transient changes in blood pressure was assessed by increasing blood pressure by 30% for one time step (6h, at tick=2, 102, 202 and 302) during a 400-time-step simulation (100 days). Also, a 1D parameter sensitivity analysis was performed to assess the ability of model to compensate for changes in pathways or behaviors. The sensitivity analysis is performed by varying a select parameter of each rule by one order of magnitude either up or down over the entire 400-time-step (100 day) simulation. Due to inherent stochasticity of the ABM, all 400-time-step simulations were replicated 5 times and the averages ± standard error are reported, unless stated otherwise.

2.4 Vascular adaptation in response to placement of a cuff

To assess the ability of the model to predict emergent behaviors in other vascular beds, we simulated the effects due to placement of a cuff around the common carotid artery (CCA). Rabbit CCA model was constructed based on information provided by Bayer et al. (1999) and Sokolis et al. (2011) regarding geometry and composition of rabbit CCA. To simulate the remodeling effects due to an adventitial cuff, with an internal pressure 7.5 kPa a radial compression of either 0, 5, or 10 percent of the CCA thickness was applied by radial displacement boundary condition in FEA.

Author Manuscript Author Manuscript Author Manuscript Author Manuscript

3 Results

3.1 Rule scoring

The rules regarding fibroblasts (Table 1, rule No. 20–25) implemented in the model scored between 5.54 and 6.18 with an average of 5.75. The lowest score belonged to production of MMP-9 by fibroblasts. The main factor contributing to the low score was lack of detailed information that would correlate amount of MMP-9 produced per single cell. Scores for all other rules can be found at Thorne et al. (2011). Therefore, all the listed rules were incorporated into the ABM.

3.2 Stability of coupled ABM-FEA model

Stability of the model was assessed with two approaches: first under normotensive conditions and second under transient (for one time step at tick = 2, 102, 202 and 302) increases in blood pressure (30% above MAP). The model was run for 400 time steps (5 repetitions) for each of these scenarios. Table 3 shows average maximum variation from the normalized initial baseline value for various parameters under normotensive conditions and transient increases in blood pressure. At tick 400, the average thickness (over the entire length) is 162.37 ± 9.32 μm (initial value = 162 μm) which indicates minor variations in thickness over time. Transient increases in blood pressure did not affect performance of the model (compared to normotensive case) (Fig. 3). Therefore, the model is capable of recovering from temporary spikes in blood pressure that may happen during intense physical activity in real life.

Although slight spatial variations are appreciated in distributions of cauchy stress, PDGF and TGF-β, the net amounts do not significantly change over the 400 tick simulations (Fig. 2). The spatial variation of TGF-β mass throughout the media is mainly due to proliferation, apoptosis and movement of SMCs, as this is the cell type that secretes TGF-β in the model. Although the distribution of PDGF appears uniform within the media over time (Fig. 2 d, e, f), subtle differences in PDGF amounts in *patches* within the media are indistinguishable because of the relatively higher production of PDGF by ECs in intima. Spatial distribution of collagen, elastin and gelatin did not change significantly during normotensive simulations (supplemental Fig. 1); the net change in mass was less than 0.01% for collagen, 0% for elastin and less than 0.01% for gelatin (average of 5 repetitions). For a complete list of figures representing spatial distribution of various proteins, please refer to supplemental Fig. 1.

3.3 Model sensitivity

Sensitivity of the model to variations in the ABM parameters was assessed by individually increasing (Table 4, X10) or decreasing (Table 4, X0.1) 16 select parameters by one order of magnitude and observing how the outputs (cell and protein content) are affected. Sensitivity of each output to these variations was determined by plotting the average ± standard error for each simulation; if the standard error values of the outputs overlap with the control, the model was considered to be not sensitive (NS) to that parameter and vice versa. Response of model to variation of these parameters can be further divided into two subcategories: stable response and unstable response. The response was considered stable if the model is capable

Author Manuscript Author Manuscript Author Manuscript Author Manuscript

of compensating for the parameter variation and establishing a new steady state, and unstable if no steady state is reached. The ABM was sensitive to 11 parameters (Table 4), and these parameters mainly belong to production of growth factors, proliferation of fibroblasts and SMCs and regulation of ECM (mainly collagen) by fibroblasts and SMCs. For example, the model was sensitive to a 10x increase of parameter m in rule no. 4 (production of TGF-β by SMCs) as shown in Supplemental Fig. 5. Within 100 days, increasing this parameter led to a 22-fold increase in TGF-β production, enhanced collagen secretion (8% at day 100) and eventually increased wall stress, but did not affect production of PDGF or proliferation of cells (Supplemental Fig. 5). Likewise, directly increasing the basal collagen secretion rate by fibroblasts (rule no. 22, Supplemental Fig.13) increased collagen mass by 3.3% after 100 days and eventually wall stress. Conversely, as shown in Fig. 4 increasing MMP-1 production by fibroblasts (rule no. 23; Fig. 4 and Supplemental Fig. 16) enhanced collagen degradation (4%), gelatin secretion (6%), metalloproteinase secretion (2%), and decreased stress (5%) in the adventitia, yet in the medial stress was increased (2.5%) along with stress-mediated production of TGF-β (2%) by SMCs and within 204 tick times a new homeostasis level was reached, whereas increased MMP-1 production by SMCs had a similar effect decreasing medial collagen (7%), wall stress (4%), growth factors, proteases, and even the number of SMCs (2%) (rule no. 5; Supplemental Fig. 6). Collectively these results highlight the role collagen regulation plays in stress-mediated remodeling of the artery. For detailed results, please refer to supplementary documents.

3.4 Vascular remodeling in response to placement of an adventitial cuff

Cuffed CCA was simulated to mimic experimental conditions of Bayer et al. (1999) using the ABM-FE framework. Placing the cuff decreased the stress in arterial wall. The decrease in stress led to a decline in cellular production of PDGF and TGF-β, decreased the population of SMCs (6%, supplemental Fig. 19j) and collagen mass (1%, supplemental Fig. 19a) and increase in gelatin mass (6%, supplemental Fig. 19f) over 400 tick times (100 days). Production of MMP-2 (33%, supplemental Fig. 19h) and 9 (8%, supplemental Fig. 19i) also decreased in response to decreased stress. These results compare to Bayer et al. (1999) who also observed a decrease in cell population and collagen mass (Bayer et al. 1999).

4 Discussion

Previously, ABM and FEA have been used separately to study various aspects of arterial remodeling, vasculogenesis and stent restenosis (Bailey et al. 2007; Bentley et al. 2008; Boyle et al. 2010); however, many of these models either neglected the role of mechanical stimuli in production of cellular proteins or take simpler approaches toward modeling the underlying biological events involved in arterial remodeling. While ABMs by Bailey et al. (2009) and Peirce et al. (2004) consider mechanical stimuli as a driving factor for production of cellular proteins, none of the existing ABMs have directly linked cellular production of growth factors and proteases with the spatial variation of arterial stress. Although Thorne et al. (2011) successfully used ABM to simulate arterial remodeling under hypertensive conditions, they used the hoop stress formula to calculate stress which assumes thin-walled tube and fails to capture any compositional or non-axisymmetric variations in stress;

Author Manuscript Author Manuscript Author Manuscript Author Manuscript

moreover, the role of adventitia and adventitial fibroblasts as active participants in maintaining homeostasis and remodeling (Gingras et al. 2009) was neglected. FEA simulations have also been used to study vascular adaptation (Sáez et al. 2014). Although these models can provide an accurate estimation of stress and strain distribution within the artery (Humphrey 2002), they often neglect biology and/or do not account for non-homogeneities of material properties or changes in geometry that develop during remodeling. In the model by Sáez et al. (2014), vascular growth is limited to the media and occurs by expansion of each element upon reaching a critical level of stretch. Herein, we improved and/or added to the previous coupled ABM-FEA models used to study vascular adaptation (including, (Zahedmanesh and Lally 2012; Boyle et al. 2013; Zahedmanesh et al. 2014; Garbey et al. 2015)) by (1) incorporating three arterial cell types, (2) including cell-specific production of growth factors and proteases and (3) accounting for the structural role of collagen, elastin and gelatin by implementing a content-based strain energy density function in the FEA. Thus, we present a coupled ABM-FEA computational framework that simulates spatiotemporal changes in geometry, composition and state of stress in response to parameter manipulation.

4.1 Stability and sensitivity of model

Maintaining homeostasis is, perhaps, the most intriguing ability of blood vessels. Despite the dynamic net of biochemo-mechanical stimuli they are exposed to, arteries are capable of withstanding temporary alterations in blood pressure and/or production of other chemical cues. Therefore, for any model to be able to predict vascular adaptation, it is first necessary to satisfy the conditions of tissue balance under normotensive conditions (i.e., balanced production and removal of constituents). The model also needs to be able to return to equilibrium after temporary increases in blood pressure or production of extracellular cytokines or growth factors. In this regard, stability of model was assessed under normotensive conditions and during transient increases in blood pressure. As expected, the results confirmed that the model is stable. We observed a dynamic response of balanced production and removal of constituents about equilibrium (Fig. 3 and Table 3). Also, the 1D parameter sensitivity analysis revealed the artery is able to compensate for changes in some parameters by reaching a new homeostatic steady state whereby the artery remodeled to accommodate for the perturbation. In summary, stability results validate that the model predicts physiological remodeling events as seen clinical normotensive control of longitudinal studies (Hayenga et al. 2013; Valentin and Humphrey 2009; Geisterfer et al. 1988). Moreover, the sensitivity studies provide insightful information about the interplay of chemical and mechanical signals in a LAD.

4.2 ECM is the key to homeostasis

The dynamic homeostatic state of the ECM proteins is a key factor in maintaining homeostasis in arterial wall (Humphrey et al. 2014), as any significant change in composition of ECM can affect the state of stress and consequently alter production of growth factors and proteases. Sensitivity studies showed that modulation of parameters involved in regulation of ECM composition, particularly collagen, had the most significant effect on the model. For instance, increasing TGF-β production by SMCs caused the net collagen mass to increase uniformly over 100 days (8% increase) and consequently

Author Manuscript Author Manuscript Author Manuscript Author Manuscript

increased the average stress (1.1%, Supplemental Fig. 5 (a)). Similar response was observed by increasing the basal rate of collagen production by fibroblasts (3.3% increase in net collagen mass, Supplemental Fig. 13) or increasing rate of collagen production by SMCs (3% increase in net collagen mass, Supplemental Fig. 11). This response is consistent with reports that hypertension can be a cause and consequence of increased blood pressure and fibrosis (Schiffrin 2012). It is worth noting that although increased collagen in the aforementioned cases led to an increase in stress, no significant change was observed in SMC population as the level of increased stress was not enough to increase PDGF production significantly.

4.3 Hyperplasia as a regulator of stress

Sensitivity studies revealed that SMC hyperplasia leads to an increase in medial thickness and decrease in stress. Increasing parameter m in rule No. 1 by fourfold led to 77% increase in SMC population (Supplemental Fig. 3) and 43% increase in thickness and decreased average maximum principal stress by 25% over the course of 100 simulated days. Hayenga et al. (2012) showed that following two weeks of hypertension, SMC population in porcine LAD increased by 33% and observations by Grinnell (1994) and Hu et al. (2008) confirm that hyperplasia can act as a regulator of stress.

4.4 Mechanical stress as a relay for chemical signals

A 10x increase in the basal production rate of MMP-1 by fibroblasts enhanced collagen degradation in the adventitia (Fig. 4), and this in turn led to a 2% decrease in overall average wall maximum principal stress and an increase in gelatin deposition. A more detailed investigation revealed that this decrease in average wall stress is mainly due to a drop in adventitial stress (5% decrease, Fig. 4a). In fact, the trend is opposite in the media, as shown in Fig. 4b, with a compensatory increase in medial stress. The increase in medial stress triggers a 2% increase in TGF-β production by SMCs (Fig. 4c) which stimulates an increase in the production of medial collagen thus compensating for the loss of collagen and stress in the adventitia. This scenario demonstrates that even though the original perturbation was chemical, it affected the mechanical stress which acted as a relay between chemical signals, triggering the secretion of proteases and growth factors in order to restore homeostasis. In previous ABMs that utilized a hoop stress formula, instead of continuum-level models, the role of ECM composition in homeostasis and signaling is ignored as stress is a purely a function of pressure and geometrical features of artery and not composition.

4.5 Atrophic remodeling in response to decreased stress

Placement of the adventitial cuff induced atrophic remodeling in the CCA model. Decreased mechanical stress at the site of the cuff led to a decrease in SMC population and collagen mass. Decrease in collagen mass was due to a decrease in collagen deposition and not degradation by MMP-1. These predictions are in accord with reports of Bayer et al. (1999) on atrophic remodeling at the site of the artery-cuffed CCA. They observed a 30% decrease in vessel wall DNA, 67 % decrease in collagen amount and 30% decrease in elastin over 21 days. They attributed the decrease in elastin mass to an increase in proteolytic activity of MMP-2 and MMP-9; however, we observed an opposite trend in our simulations as production of MMP-2 and 9 in existing rules is a monotonic function of stress (rules 6, 7).

Author Manuscript Author Manuscript Author Manuscript Author Manuscript

This trend suggested a shift in our understanding, in that low levels of stress may actually increase the production of MMP-2 and 9.

4.6 Limitations

The arterial wall constituents are assumed to be isotropic materials and collagen fiber anisotropy is neglected, and this simplification was mainly due to lack of information about the evolution of collagen fiber direction during remodeling process. Moreover, experiments by other researchers (Wang et al. 2006) have shown that anisotropic behavior of collagen in a porcine LAD is most significant at circumferential strain values above 20%; these strain values are typically observed when the mean arterial blood pressure is elevated by $>30\%$. Therefore, the model is particularly useful under cases of significant remodeling or for simulating changes as a result of MAP $<30\%$ where fiber alignment is less crucial. Similar to collagen, active material properties of SMCs add anisotropy to the material model and regulate the mechanical response of arteries. However, to implement anisotropy in strain energy density functions we need to know the orientations of SMCs during migration, proliferation and remodeling. Therefore, we neglected their active properties, but implemented their passive mechanical properties. It would be possible to include active properties, but we would need to assume that they maintain their orientations during remodeling. Similarly, the role of residual stress in arterial adaptation is ignored as the goal of this model is to predict stress and strain values during remodeling, and published spatiotemporal dependent measures of opening angle and axial prestretch values during remodeling do not exist. Blood pressure is pulsatile in nature; however, for simplicity we assumed it to be constant and equal to mean arterial pressure. This approach should give the appropriate average response, as well as many of the rules were based on average stress or strain deformations. Even though kinetics of MMP, proMMP and tissue inhibitor of metalloproteinase (TIMP) have been investigated by various researchers using Michaelis–Menten reaction scheme (Karagiannis and Popel 2004, 2006; Vempati et al. 2007), in this model we did not account for role of TIMPs and proMMPs in kinetic of MMP activation/inhibition and regulation of ECM content. This omission was mainly due to the lack of appropriate experimental data on their per cell production rates and the uncertain complexity of MMP–proMMP–TIMP interactions (Karagiannis and Popel 2006). However, the model accounts for the effects of TIMPs via the MMP removal rules 17, 18 and 19. An advantage to ABM is the ability to refine and substitute/expand rules as the relationship become more known. Despite an incremental increase of collagen, in response to increased levels of TGF-β (supplemental Fig 5) or decreased secretion of MMP-1, average stress only increased after 330 time steps. One factor contributing to this delayed response is the method implemented in ABM for passing the mechanical properties to FEA which requires a 5% change in mass fraction of a content within each patch to update the material. Clustering techniques, such as k-means method (Kanungo et al. 2002), can be an alternative to the predefined material table, and these techniques will allow the model to account for incremental variations in mechanical properties by identifying patches with similar combination of the four contents and forming clusters that each represents one material. However, this increased accuracy comes at the cost of increased computational cost. Albeit we preformed gross validation of the model, under normotensive conditions and in the case of an arterial cuff, we did not validate the parameter sensitivity predictions. To validate the sensitivity studies, we desire in

Author Manuscript Author Manuscript Author Manuscript Author Manuscript

vivo or ex vivo experimental data that show how a change in the concentration of a macromolecule (e.g., MMP, TGF-β, PDGF) affects the stress level, constituents and soluble factors in the artery wall. Currently, these type of experiments do not exist, and in the case of knockout (KO) mouse models, the coronary arteries are not investigated. Therefore, currently, many of the model predictions cannot be quantitatively validated; however, these predictions provide insightful information for designing future experiments and help close the gap between in vitro experiments and observed phenomenon.

In summary, we have developed a coupled ABM-FEA model of arterial adaptation. Coupling microscale changes in cytokines, growth factors and proteases to macroscale changes in geometry, composition and stress distribution allows this model to capture emergent behaviors in arterial adaptation and has the potential to decrease the economic burden of hypertension and other arterial pathologies by facilitating management of their complications and discovery of new therapeutic agents.

Supplementary Material

Refer to Web version on PubMed Central for supplementary material.

Acknowledgements

The authors acknowledge the financial support for this work provided by the University of Texas at Dallas (startup funds to HNH) and the American Heart Association (Scientist Development Grant 17SDG33400239 to HNH). We would like to thank UT Dallas undergraduate Ramya Akkala and graduate student Rita Bhui for their assistance in scoring the ABM rules.

References

Absood A (2004) A comparison of oxidized LDL-induced collagen secretion by graft and aortic SMCs: role of PDGF. AJP Heart Circ Physiol 287(3):H1200–H1206. doi:10.1152/ajpheart.00228.2004

Aromatario C, Sterpetti AV, Palumbo R, Patrizi AL, Di Carlo A, Proietti P, Guglielmi MB, Cavallaro A, Santoro-D'Angelo L, Cucina A (1997) Fluid shear stress increases the release of platelet derived growth factor BB (PDGF BB) by aortic endothelial cells. Minerva Cardioangiol 45(1–2):1–7 [PubMed: 9167422]

Bailey AM, Thorne BC, Peirce SM (2007) Multi-cell agent-based simulation of the microvasculature to study the dynamics of circulating inflammatory cell trafficking. Ann Biomed Eng 35(6):916–936. doi:10.1007/s10439-007-9266-1 [PubMed: 17436112]

Bailey AM, Lawrence MB, Shang H, Katz AJ, Peirce SM (2009) Agent-based model of therapeutic adipose-derived stromal cell trafficking during ischemia predicts ability to roll on p-selectin. PLoS Comput Biol. doi:10.1371/journal.pcbi.1000294

Bayer IM, Adamson SL, Langille BL (1999) Atrophic remodeling of the artery-cuffed artery. Arterioscler Thromb Vasc Biol 19(6):1499–1505. doi:10.1161/01.ATV.19.6.1499 [PubMed: 10364081]

Bentley K, Gerhardt H, Bates PA (2008) Agent-based simulation of notch-mediated tip cell selection in angiogenic sprout initialisation. J Theor Biol 250(1):25–36. doi:10.1016/j.jtbi.2007.09.015 [PubMed: 18028963]

Boyle CJ, Lennon AB, Early M, Kelly DJ, Lally C, Prendergast PJ (2010) Computational simulation methodologies for mechanobiological modelling: a cell-centred approach to neointima development in stents. Phil Trans R Soc A 368:2919–2935. doi:10.1098/rsta.2010.0071 [PubMed: 20478914]

Author Manuscript Author Manuscript Author Manuscript Author Manuscript

Boyle CJ, Lennon AB, Prendergast PJ (2013) Application of a mechanobiological simulation technique to stents used clinically. J Biomech 46(5):918–924. doi:10.1016/j.jbiomech.2012.12.014 [PubMed: 23398970]

Chamley-Campbell J, Campbell GR, Ross R (1979) The smooth muscle cell in culture. Physiol Rev 59(1):1–61 [PubMed: 108688]

Chapman GB, Durante W, Hellums JD, Schafer aI (2000) Physiological cyclic stretch causes cell cycle arrest in cultured vascular smooth muscle cells. Am J Physiol Heart Circ Physiol 278(3):H748–54 [PubMed: 10710342]

Cockrell RC, Christley S, Chang E, An G (2015) Towards anatomic scale agent-based modeling with a massively parallel spatially explicit general-purpose model of enteric tissue (SEGMEnT-HPC). PLoS ONE 10(3):1–14. doi:10.1371/journal.pone.0122192

Dancu MB (2004) Asynchronous shear stress and circumferential strain reduces endothelial NO synthase and cyclooxygenase-2 but induces endothelin-1 gene expression in endothelial cells. Arterioscler Thromb Vasc Biol 24(11):2088–2094. doi:10.1161/01.ATV.0000143855.85343.0e [PubMed: 15345505]

Das M, Bouchey DM, Moore MJ, Hopkins DC, Nemenoff RA, Stenmark KR (2001) Hypoxia-induced proliferative response of vascular adventitial fibroblasts is dependent on g protein-mediated activation of mitogen-activated protein kinases. J Biol Chem 276(19):15631–15640. doi:10.1074/jbc.M010690200 [PubMed: 11278727]

Engler AJ, Griffin MA, Sen S, Bönnemann CG, Sweeney HL, Discher DE (2004) Myotubes differentiate optimally on substrates with tissue-like stiffness. J Cell Biol 166(6):877–887. doi:10.1083/jcb.200405004 [PubMed: 15364962]

Ethier MF, Hickler RB, Saunders RH (1982) Cholesterol and cholesteryl ester concentration in different size classes of cultured human fibroblasts: effect of in vitro aging. Mech Ageing Dev 20(2):165–174. doi:10.1016/0047-6374(82)90067-7 arXiv:1011.1669v3 [PubMed: 7176708]

Fridez P, Makino A, Kakoi D, Miyazaki H, Meister JJ, Hayashi K, Stergiopulos N (2002) Adaptation of conduit artery vascular smooth muscle tone to induced hypertension. Ann Biomed Eng 30(7):905–916. doi:10.1114/1.1507326 [PubMed: 12398421]

Garbey M, Rahman M, Berceli S (2015) A multiscale computational framework to understand vascular adaptation. J Comput Sci 8:32–47. doi:10.1016/j.jocs.2015.02.002 [PubMed: 25977733]

Garcia-Lopez G, Vadillo-Ortega F, Merchant-Larios H, Maida-Claros R, Osorio M, Soriano-Becerril D, Flores-Herrera H, Beltran-Montoya J, Garfias-Becerra Y, Zaga-Clavellina V (2007) Evidence of in vitro differential secretion of 72 and 92 kDa type IV collagenases after selective exposure to lipopolysaccharide in human fetal membranes. Mol Hum Reprod 13(6):409–418. doi:10.1093/molehr/gam025 [PubMed: 17449536]

Garipcan B, Maenz S, Pham T, Settmacher U, Jandt KD, Zanow J, Bossert J (2011) Image analysis of endothelial microstructure and endothelial cell dimensions of human arteries–a preliminary study. Adv Eng Mater 13(1–2):54–57. doi:10.1002/adem.201080076

Geisterfer AA, Peach MJ, Owens GK (1988) Angiotensin ii induces hypertrophy, not hyperplasia, of cultured rat aortic smooth muscle cells. Circ Res 62(4):749–756 [PubMed: 3280155]

Gingras M, Farand P, Safar ME, Plante GE (2009) Adventitia: the vital wall of conduit arteries. J Am Soc Hypertens 3(3):166–183. doi:10.1016/j.jash.2009.03.002 [PubMed: 20409958]

Grinnell F (1994) Fibroblasts, myofibroblasts, and wound contraction. J Cell Biol 124(4):401–404 [PubMed: 8106541]

Guo X, Liu Y, Kassab GS (2012) Diameter-dependent axial prestretch of porcine coronary arteries and veins. J Appl Physiol 112(6):982–989. doi:10.1152/japplphysiol.00857.2011 [PubMed: 22162531]

Hayashi K, Naiki T (2009) Adaptation and remodeling of vascular wall; biomechanical response to hypertension. J Mech Behav Biomed Mater 2(1):3–19. doi:10.1016/j.jmbbm.2008.05.002 [PubMed: 19627803]

Hayenga HN, Thorne BC, Peirce SM, Humphrey JD (2011) Ensuring congruency in multiscale modeling: towards linking agent based and continuum biomechanical models of arterial adaptation. Ann Biomed Eng 39(11):2669–2682. doi:10.1007/s10439-011-0363-9 [PubMed: 21809144]

Author Manuscript Author Manuscript Author Manuscript Author Manuscript

Hayenga HN, Hu JJ, Meyer CA, Wilson E, Hein TW, Kuo L, Humphrey JD (2012) Differential progressive remodeling of coronary and cerebral arteries and arterioles in an aortic coarctation model of hypertension. Front Physiol. doi:10.3389/fphys.2012.00420

Hayenga HN, Thorne BC, Yen P, Papin JA, Peirce SM, Humphrey JD (2013) Multiscale computational modeling in vascular biology: from molecular mechanisms to tissue-level structure and function In: Multiscale computer modeling in biomechanics and biomedical engineering SE - 147, vol 14, pp 209–240, doi:10.1007/8415_2012_147

Hsieh HJ, Li NQ, Frangos Ja (1991) Shear stress increases endothelial platelet-derived growth factor mRNA levels. Am J Physiol 260(2 Pt 2):H642–6 [PubMed: 1996708]

Hu JJ, Ambrus A, Fossum TW, Miller MW, Humphrey JD, Wilson E (2008) Time courses of growth and remodeling of porcine aortic media during hypertension: a quantitative immunohistochemical examination. J Histochem Cytochem 56(4):359–370 [PubMed: 18071063]

Humphrey JD (2002) Cardiovascular solid mechanics, vol 1 Springer, New York. doi: 10.1007/978-0-387-21576-1

Humphrey JD, Dufresne ER, Schwartz Ma (2014) Mechanotransduction and extracellular matrix homeostasis. Nat Rev Mol Cell Biol 15(12):802–812, doi:10.1038/nrm3896 [PubMed: 25355505]

Intengan HD, Schiffrin EL (2001) Vascular remodeling in hypertension. Hypertension 38(3):581–587. doi:10.1161/hy09t1.096249 [PubMed: 11566935]

Jenkins C, Milsted A, Doane K, Meszaros G, Toot J, Ely D (2007) A cell culture model using rat coronary artery adventitial fibroblasts to measure collagen production. BMC Cardiovasc Disord 7(1):13. doi:10.1186/1471-2261-7-13 [PubMed: 17488510]

Kanai AJ, Strauss HC, Truskey GA, Crews AL, Grunfeld S, Malinski T (1995) Shear stress induces ATP-independent transient nitric oxide release from vascular endothelial cells, measured directly with a porphyrinic microsensor. Circ Res 77(2):284–293. doi:10.1161/01.RES.77.2.284 [PubMed: 7614715]

Kanungo T, Mount D, Netanyahu N, Piatko C, Silverman R, Wu A (2002) An efficient k-means clustering algorithm: analysis and implementation. IEEE Trans Pattern Anal Mach Intell 24(7): 881–892, doi:10.1109/TPAMI.2002.1017616, arXiv:0711.0189v1

Karagiannis ED, Popel AS (2004) A theoretical model of type I collagen proteolysis by matrix metalloproteinase (mmp) 2 and membrane type 1 mmp in the presence of tissue inhibitor of metalloproteinase 2. J Biol Chem 279(37):39105–39114. doi:10.1074/jbc.M403627200 [PubMed: 15252025]

Karagiannis ED, Popel AS (2006) Distinct modes of collagen type i proteolysis by matrix metalloproteinase (mmp) 2 and membrane type i mmp during the migration of a tip endothelial cell: insights from a computational model. J Theor Biol 238(1):124–145. doi:10.1016/j.jtbi. 2005.05.020 [PubMed: 16005020]

Karakiulakis G, Papakonstantinou E, Aletras AJ, Tamm M, Roth M (2007) Cell type-specific effect of hypoxia and platelet-derived growth factor-BB on extracellular matrix turnover and its consequences for lung remodeling. J Biol Chem 282(2):908–915. doi:10.1074/jbc.M602178200 [PubMed: 17099219]

Karšaj I, Humphrey JD (2012) A multilayered wall model of arterial growth and remodeling. Mech Mater 44:110–119. doi:10.1016/j.mechmat.2011.05.006 [PubMed: 22180692]

Karšaj I, Sorić J, Humphrey J (2010) A 3-D framework for arterial growth and remodeling in response to altered hemodynamics. Int J Eng Sci 48(11):1357–1372. doi:10.1016/j.ijengsci.2010.06.033 [PubMed: 21218158]

Kim YJ, Sah RL, Doong JY, Grodzinsky aJ (1988) Fluorometric assay of DNA in cartilage explants using Hoechst 33258. Anal Biochem 174(1):168–176. doi:10.1016/0003-2697(88)90532-5 [PubMed: 2464289]

Kim DK, Huh JE, Lee SH, Hong KP, Park JE, Seo JD, Lee WR (1999) Angiotensin II stimulates proliferation of adventitial fibroblasts cultured from rat aortic explants. J Korean Med Sci 14(5): 487. doi:10.3346/jkms.1999.14.5.487 [PubMed: 10576143]

Kim YS, Galis ZS, Rachev A, Han HC, Vito RP (2009) Matrix metalloproteinase-2 and −9 are associated with high stresses predicted using a nonlinear heterogeneous model of arteries. J Biomech Eng 131(1):011009. doi:10.1115/1.3005163 [PubMed: 19045925]

Author Manuscript Author Manuscript Author Manuscript Author Manuscript

Korshunov VA, Schwartz SM, Berk BC (2007) Vascular remodeling: hemodynamic and biochemical mechanisms underlying Glagov's phenomenon. Arterioscle Thromb Vasc Biol 27(8):1722–1728. doi:10.1161/ATVBAHA.106.129254

Lê J, Dauchot P, Perrot JL, Cambazard F, Frey J, Chamson A (1999) Quantitative zymography of matrix metalloproteinases by measuring hydroxyproline: Application to gelatinases A and B. Electrophoresis 20(14):2824–2829. doi:10.1002/(SICI)1522-2683(19991001)20:14<2824::AID-ELPS2824>3.0.CO;2-H [PubMed: 10546813]

Lefevre M, Rucker RB (1980) Aorta elastin turnover in normal and hypercholesterolemic Japanese quail. Biochim Biophys Acta 630(4):519–529. doi:10.1016/0304-4165(80)90006-9 [PubMed: 6772235]

Li Z, Moore S, Alavi MZ (1995) Mitogenic factors released from smooth muscle cells are responsible for neointimal cell proliferation after balloon catheter deendothelialization. Exp Mol Pathol 63(2): 77–86. doi:10.1006/exmp.1995.1032 [PubMed: 8941042]

Lou X (1999) Swelling behavior and mechanical properties of chemically cross-linked gelatin gels for biomedical use. J Biomater Appl. doi:10.1177/088532829901400204

Lu Q, Ganesan K, Simionescu DT, Vyavahare NR (2004) Novel porous aortic elastin and collagen scaffolds for tissue engineering. Bio-materials 25(22):5227–5237. doi:10.1016/j.biomaterials.2003.12.019

Ma YH, Ling S, Ives HE (1999) Mechanical strain increases PDGF-B and PDGF β receptor expression in vascular smooth muscle cells. Biochem Biophys Res Commun 265(2):606–610. doi:10.1006/bbrc.1999.1718 [PubMed: 10558917]

Mata-Greenwood E (2005) Cyclic stretch increases VEGF expression in pulmonary arterial smooth muscle cells via TGF-1 and reactive oxygen species: a requirement for NAD(P)H oxidase. AJP Lung Cell Mol Physiol 289(2):L288–L289. doi:10.1152/ajplung.00417.2004

Morishita R, Gibbons GH, Horiuchi M, Kaneda Y, Ogihara T, Dzau VJ (1998) Role of AP-1 complex in angiotensin II-mediated transforming growth factor-β expression and growth of smooth muscle cells: using decoy approach against AP-1 binding site. Biochem Biophys Res Commun 243(2): 361–367. doi:10.1006/bbrc.1997.8012 [PubMed: 9480814]

Murphy G, McAlpine CG, Poll CT, Reynolds JJ (1985) Purification and characterization of a bone metalloproteinase that degrades gelatin and types IV and V collagen. Biochim et Biophys Acta (BBA) Protein Struct Mol Enzymol 831(1):49–58. doi:10.1016/0167-4838(85)90148-7

Norris TO, McGraw J (1964) Gelatin coatings and tensile strength of gelatin films. J Appl PolymSci 8(5):2139–2145. doi:10.1002/app.1964.070080514

North MJ, Collier NT, Ozik J, Tatara ER, Macal CM, Bragen M, Sydelko P (2013) Complex adaptive systems modeling with repast simphony. Complex Adapt Syst Model 1(1):1–26. doi:10.1186/2194-3206-1-3

Okuno T, Andoh A, Bamba S, Araki Y, Fujiyama Y, Fujimiya M, Bamba T (2002) Interleukin-1β and tumor necrosis factor-α induce chemokine and matrix metalloproteinase gene expression in human colonic subepithelial myofibroblasts. Scand J Gastroenterol 37(3):317–324. doi:10.1080/003655202317284228 [PubMed: 11916194]

Owens GK, Rabinovitch PS, Schwartz SM (1981) Smooth muscle cell hypertrophy versus hyperplasia in hypertension. Proc Natl Acad Sci 78(12):7759–7763. doi:10.1073/pnas.78.12.7759 [PubMed: 6950415]

Peirce SM, Van Gieson EJ, Skalak TC (2004) Multicellular simulation predicts microvascular patterning and in silico tissue assembly. FASEB J Off Publ Fed Am Soc Exp Biol 18(6):731–733. doi:10.1096/fj.03-0933fje

Qiu H, Zhu Y, Sun Z, Trzeciakowski JP, Gansner M, Depre C, Resuello RRG, Natividad FF, Hunter WC, Genin GM, Elson EL, Vatner DE, Meininger GA, Vatner SF (2010) Short communication: vascular smooth muscle cell stiffness as a mechanism for increased aortic stiffness with aging. Circ Res 107(5):615–619. doi:10.1161/CIRCRESAHA.110.221846 [PubMed: 20634486]

Reidy MA (1994) Growth factors and arterial smooth muscle cell proliferationa. Ann N Y Acad Sci 714(1):225–230. doi:10.1111/j.1749-6632.1994.tb12047.x [PubMed: 8017771]

Author Manuscript Author Manuscript Author Manuscript Author Manuscript

Sáez P, Peña E, Martínez MA, Kuhl E (2014) Computational modeling of hypertensive growth in the human carotid artery. Comput Mech 53(6):1183–1196. doi:10.1007/s00466-013-0959-z [PubMed: 25342868]

Schiffrin EL (2012) Vascular remodeling in hypertension: mechanisms and treatment. Hypertension 59(2):367–374. doi:10.1161/HYPERTENSIONAHA.111.187021 [PubMed: 22203749]

Schlumberger W, Thie M, Rauterberg J, Robenek H (1991) Collagen synthesis in cultured aortic smooth muscle cells. Modulation by collagen lattice culture, transforming growth factor-beta 1, and epidermal growth factor. Arterioscle Thromb Vasc Biol 11(6):1660–1666. doi: 10.1161/01.ATV.11.6.1660

Sokolis DP, Sassani S, Kritharis EP, Tsangaris S (2011) Differential histomechanical response of carotid artery in relation to species and region: mathematical description accounting for elastin and collagen anisotropy. Med Biol Eng Comput 49(8):867–879. doi:10.1007/s11517-011-0784-5 [PubMed: 21626234]

Stegemann JP, Nerem RM (2003) Altered response of vascular smooth muscle cells to exogenous biochemical stimulation in two- and three-dimensional culture. Exp Cell Res 283(2):146–155. doi: 10.1016/S0014-4827(02)00041-1 [PubMed: 12581735]

Stroka KM, Aranda-Espinoza H (2011) Endothelial cell substrate stiffness influences neutrophil transmigration via myosin light chain kinase-dependent cell contraction. Blood 118(6):1632–1640. doi:10.1182/blood-2010-11-321125 [PubMed: 21652678]

Thorne BC, Hayenga HN, Humphrey JD, Peirce SM (2011) Toward a multi-scale computational model of arterial adaptation in hyperten sion: verification of a multi-cell agent-based model. Front Physiol. doi:10.3389/fphys.2011.00020

Valentin A, Humphrey J (2009) Evaluation of fundamental hypotheses underlying constrained mixture models of arterial growth and remodelling. Philos Trans R Soc Lond A Math Phys Eng Sci 367(1902):3585–3606. doi:10.1098/rsta.2009.0113

van den Broek CN, Van der Horst A, Rutten MC, Van De Vosse FN (2011) A generic constitutive model for the passive porcine coronary artery. Biomech Model Mechanobiol 10(2):249–258. doi: 10.1007/s10237-010-0231-9 [PubMed: 20556629]

Vempati P, Karagiannis ED, Popel AS (2007) A biochemical model of matrix metalloproteinase 9 activation and inhibition. J Biol Chem 282(52):37585–37596. doi:10.1074/jbc.M611500200 [PubMed: 17848556]

Wang C, Garcia M, Lu X, Lanir Y, Kassab GS (2006) Three-dimensional mechanical properties of porcine coronary arteries: a validated two-layer model. Am J Phys Heart Circ Phys 291(3):H1200–9. doi:10.1152/ajpheart.01323.2005

Welgus HG, Jeffrey JJ, Stricklin GP, Roswit WT, Eisen aZ (1980) Characteristics of the action of human skin fibroblast collagenase on fibrillar collagen. J Biol Chem 255(14):6806–6813 [PubMed: 6248534]

Welgus HG, Jeffrey JJ, Eisen aZ (1981) The collagen substrate specificity of human skin fibroblast collagenase. J Biol Chem 256(18):9511–9515 [PubMed: 6270089]

Wilensky U, Evanston I (1999) NetLogo: center for connected learning and computer-based modeling. Northwestern University, Evanston

Wu J, Thabet SR, Kirabo A, Trott DW, Saleh MA, Xiao L, Madhur MS, Chen W, Harrison DG (2014) Inflammation and mechanical stretch promote aortic stiffening in hypertension through activation of p38 mitogen-activated protein kinase. Circ Res 114(4):616–625. doi:10.1161/CIRCRESAHA.114.302157 [PubMed: 24347665]

Xia T, Akers K, Eisen AZ, Seltzer JL (1996) Comparison of cleavage site specificity of gelatinases A and B using collagenous peptides. Biochim et Biophys Acta (BBA) Protein Struct Mol Enzymology 1293(2):259–266. doi:10.1016/0167-4838(95)00259-6

Yakimets I, Wellner N, Smith AC, Wilson RH, Farhat I, Mitchell J (2005) Mechanical properties with respect to water content of gelatin films in glassy state. Polymer 46(26):12577–12585. doi: 10.1016/j.polymer.2005.10.090

Zahedmanesh H, Lally C (2012) A multiscale mechanobiological modelling framework using agent-based models and finite element analysis: application to vascular tissue engineering. Biomech Model Mechanobiol 11(3–4):363–77. doi:10.1007/s10237-011-0316-0 [PubMed: 21626394]

Author Manuscript Author Manuscript Author Manuscript Author Manuscript

Zahedmanesh H, Van Oosterwyck H, Lally C (2014) A multi-scale mechanobiological model of in-stent restenosis: deciphering the role of matrix metalloproteinase and extracellular matrix changes. Comput Methods Biomech Biomed Eng. doi:10.1080/10255842.2012.716830

Ziegler T, Bouzourene K, Harrison VJ, Brunner HR, Hayoz D (1998) Influence of oscillatory and unidirectional flow environments on the expression of endothelin and nitric oxide synthase in cultured endothelial cells. Arterioscler Thromb Vasc Biol 18(5):686–692. doi:10.1161/01.ATV.18.5.686 [PubMed: 9598825]

Zulliger Ma, Fridez P, Hayashi K, Stergiopulos N (2004) A strain energy function for arteries accounting for wall composition and structure. J Biomech 37(7):989–1000. doi:10.1016/j.jbiomech.2003.11.026 [PubMed: 15165869]

Author Manuscript Author Manuscript Author Manuscript Author Manuscript

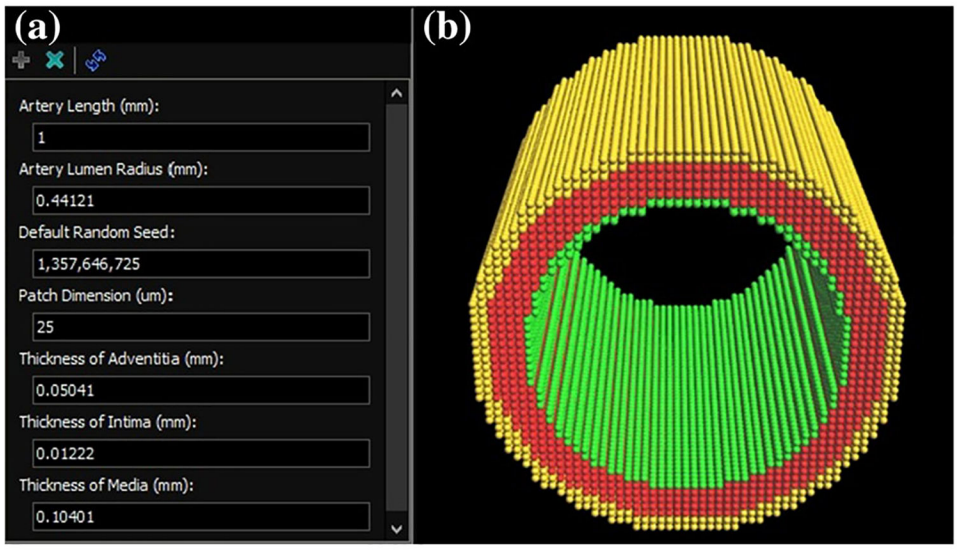

Fig. 1.

Schema of the agent-based model and GUI. **a** The GUI allows for defining blood vessel geometry. **b** Spheres represent cells within the ABM; *green spheres* are ECs, *red spheres* are SMCs, and *yellow spheres* are AFs

Author Manuscript Author Manuscript Author Manuscript Author Manuscript

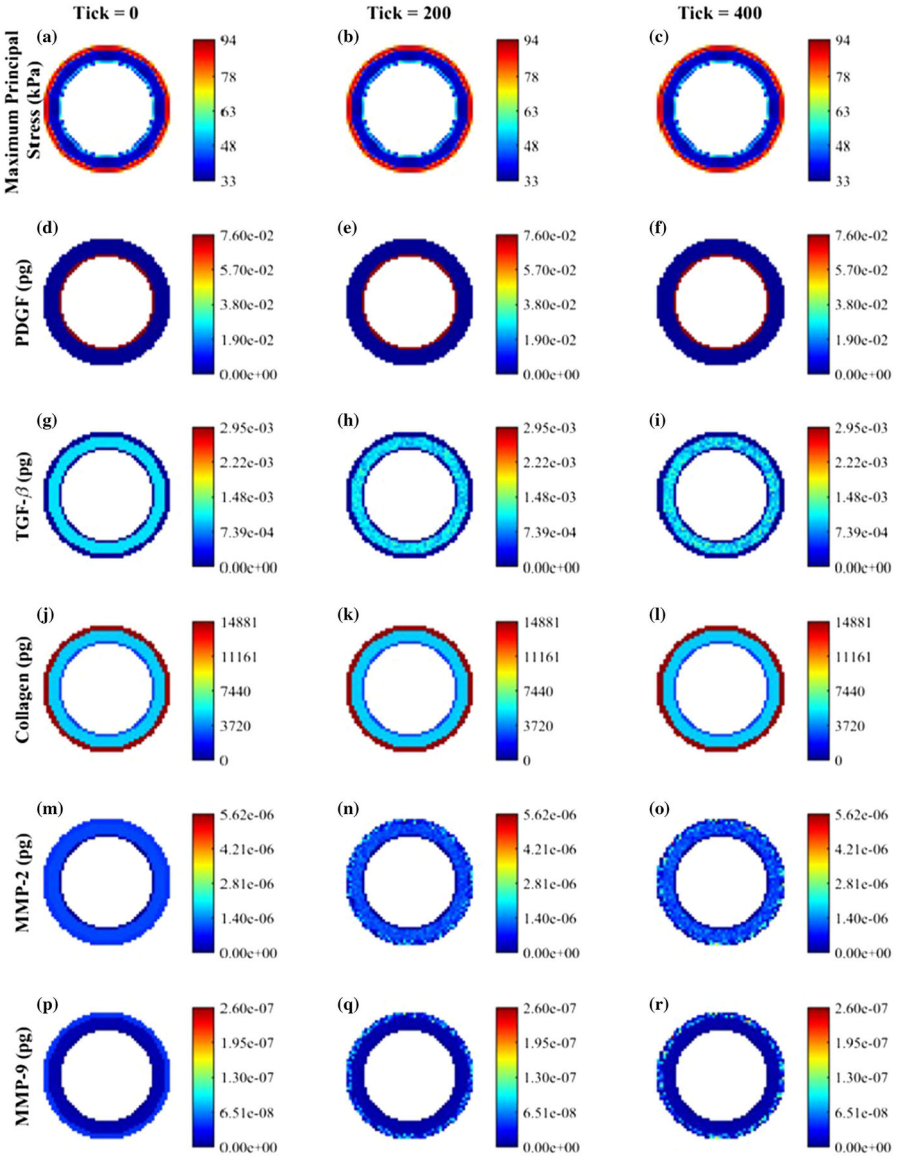

Fig. 2.

Evolution of maximum principal stress (kPa), amounts per patch of PDGF-AB (pg), TGF-β (pg), collagen (pg), MMP-2 (pg) and MMP-9 (pg) in porcine LAD under normotensive conditions. Values are plotted at tick times of 0 (initial), 200 (50 days) and 400 (100 days) at each patch in a cross section at the middle of the artery. Variation of PDGF-AB and TGF-β is minimal under normotensive conditions

Author Manuscript Author Manuscript Author Manuscript Author Manuscript

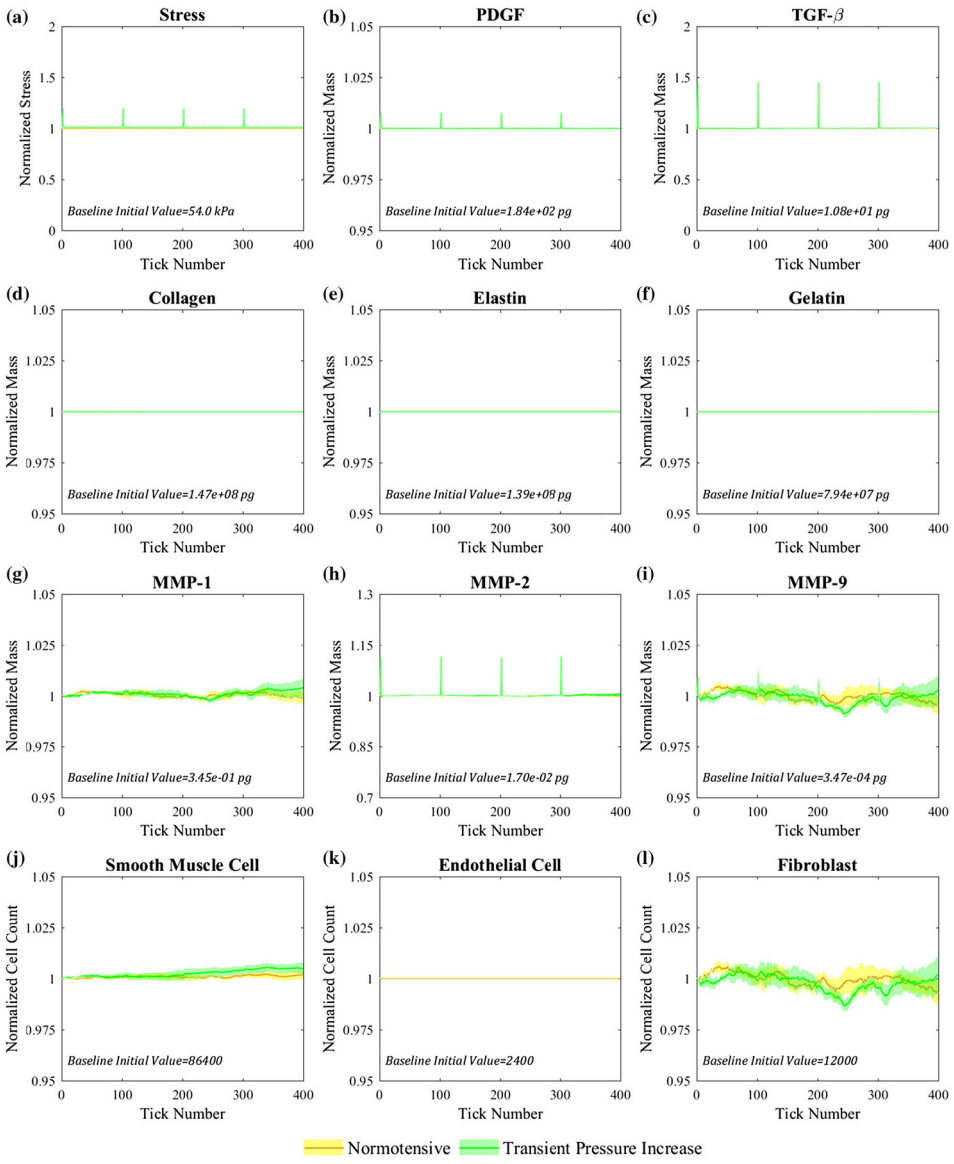

Fig. 3.

Effect of transient periodic increases in blood pressure on **a** average maximum principal stress, **b**, **c** growth factors, **d–f** structurally significant proteins of ECM, **g–i** proteases and **j–l** cell population. All values are normalized to initial baseline value. Blood pressure was increased by 30% for one time step (6h) at tick = 2, 102, 202 and 302 and results (average (*solid line*) standard error (*shaded region*)) were plotted against that of normotensive conditions. No significant change was observed in any of the parameters

Author Manuscript Author Manuscript Author Manuscript Author Manuscript

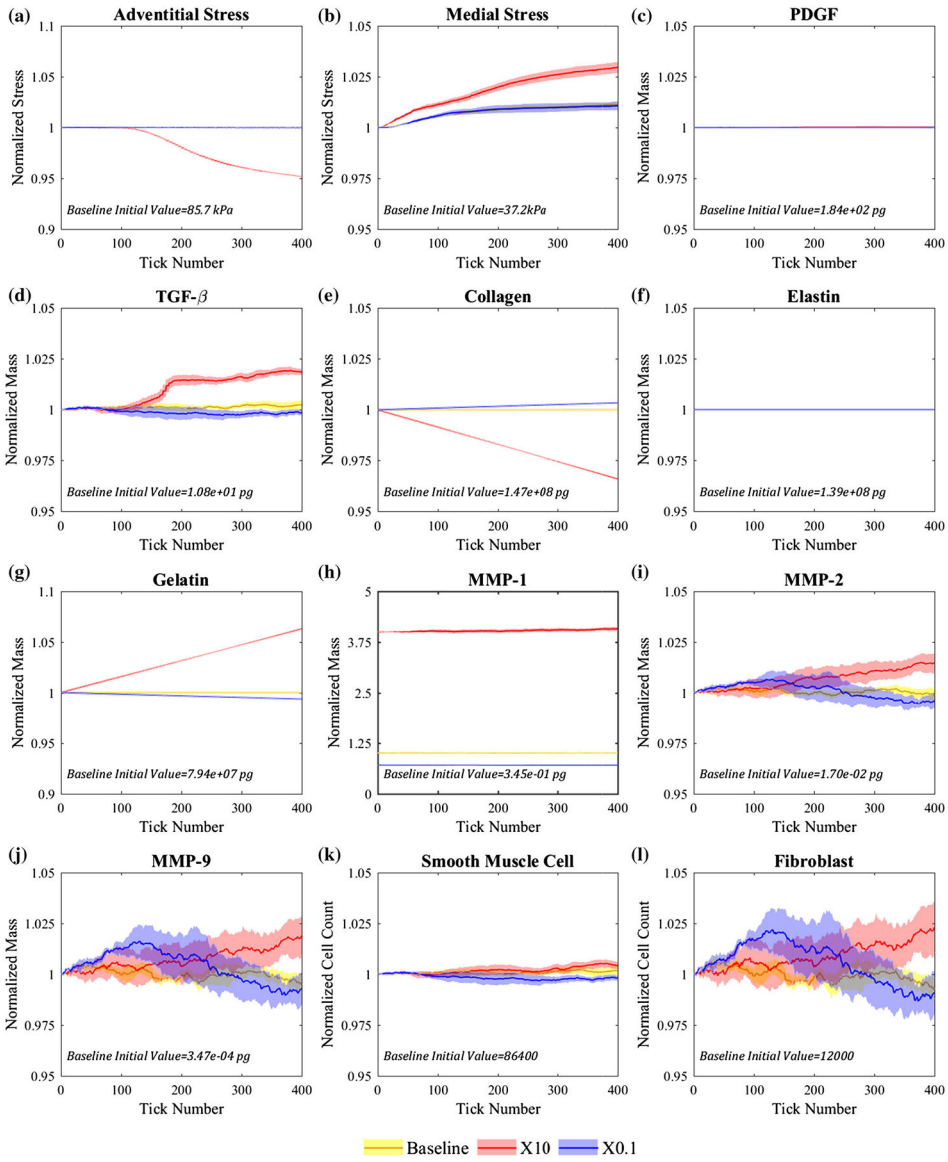

Fig. 4.

Effect of varying parameter b in rule No. 23 (production of MMP-1 by fibroblasts) on **a**, **b** average adventitial and medial maximum principal stress, **c**, **d** growth factors, **e**–**g** structurally significant proteins of ECM, **h**, **i** proteases and **k**, **l** cell population. All values are normalized to initial baseline value. Parameter b was increased and decreased by an order of magnitude as shown in (h). Increased MMP-1 production in adventitia enhanced collagen degradation, decreased average maximum principal stress and eventually led to higher TGF-β production by SMCs

Author Manuscript Author Manuscript Author Manuscript Author Manuscript

Table 1

List of rules implemented in the ABM

Rule no.	Behavior	ABM rule	References
1	SMC proliferation chance	16.67/($m \times PDGF + b$) (h^{-1}) m = − 14.54e8($pg^{-1}h$) b = 8.0e4 (h)	Reidy (1994), Chapman et al. (2000) and Stegemann and Nerem (2003)
2	SMC apoptosis chance	2.35 e−4(h^{-1})	MBC[a]
3	SMC production of PDGF-AB (stretch induced)	$PDGF = m \times \sigma + b$(pg $Cell^{-1}h^{-1}$) $m = 7.98e - 08$(pg$Cell^{-1}h^{-1}kPa^{-1}$) $b = 6.95e - 06$(pg$Cell^{-1}h^{-1}$)	Li et al. (1995) and Ma et al. (1999)
4	SMC production of TGF-β (stretch induced)	$TGF\beta = m \times \sigma + b$(pg $Cell^{-1}h^{-1}$) $m = 2.76e - 7$(pg $Cell^{-1}h^{-1}kPa^{-1}$) $b = -1.72e - 5$(pg$Cell^{-1}h^{-1}$)	Morishita et al. (1998) and Mata-Green wood (2005)
5	SMC production of MMP-1 (constant)	MMP1 = $b \times a$ (pg $Cell^{-1}h^{-1}$) $b = 4.50e - 5$ (pg $Cell^{-1}h^{-1}$), $a = 39.32\%$ (percent active)	Owens et al. (1981) and Karakiulakis et al. (2007)
6	SMC production of MMP-2 (stretch induced)	MMP2 $= A \times M(\delta + \alpha(1 - \exp(-(\sigma/\kappa)^n)))$ $A = 0.003$ (% active), $M = 0.1667$ (pg $Cell^{-1}h^{-1}$) (maximum rate), $\delta = 0.03$. $\alpha = 0.52$, $\kappa = 101.55$(kPa), $n = 2.84$	Okuno et al. (2002) and Kim et al. (2009)
7	SMC production of MMP-9 (stretch induced)	MMP9 = $A \times M(\delta + \alpha\ (1 - \exp(-(\sigma/\kappa)^n)))$ $A = 0.003$, (% active) $M = 0.0003$ (pg $Cell^{-1}h^{-1}$) (maximum rate), $\delta = 0.04$, $\alpha = 0.44$. $\kappa = 78.87$(kPa), $n = 2.88$	Garcia-Lopez et al. (2007) and Kim et al. (2009)
8	SMC production of Collagen (TGF-β dependent)	if $TG\beta > 0$ & $PDGF > 0$: $m \times TGF\beta + b$ $m = 19.16$(pg $Cell^{-1}$ h^{-1}) b=14.98$e - 4$ ($Cell^{-1}h^{-1}$) Otherwise: basal production = b(pg $Cell^{-1}$ h^{-1})	Kim et al. (1988), Schlumberger et al. (1991) and Absood (2004)
9	EC production of NO (flow induced)	$\tilde{\tau}_W = 0$, $NO = 0$ $0 < \tilde{\tau}_W < 1$, $NO = 0.5$ $\tilde{\tau}_W \geq 1$, $NO = m\tilde{\tau}_W + b$ $\tilde{\tau}_W = \tilde{\tau}_W^{\text{mouse}} - \left(\tilde{\tau}_{wh}^{\text{mouse}} - \tilde{\tau}_{wh}^{\text{BAEC}}\right)$ $m = 1.092$(pmol/sec), $b = 0.87$ (pmol/sec)	Kanai et al. (1995)
10	EC production of PDGF-AB (flow induced)	$M(\delta + \alpha(1 - \exp(-(\tau_W/\kappa)^n)))$ $M = 0.104$ (pg $Cell^{-1}$ h^{-1}) (maximum rate) $\delta = 0.15$, $\alpha = 0.84$, $\kappa = 2.01$ (Pa), $n = 1.24$	Hsieh et al. (1991) and Aromatario et al. (1997)
11	EC production of ET-1 (flow induced)	$M(\delta + \alpha(1 - \exp(-(\tau_W/\kappa)^n)))$	Ziegler et al. (1998) and Dancu (2004)

Author Manuscript Author Manuscript Author Manuscript Author Manuscript

Rule no.	Behavior	ABM rule	References
		$M = 6.40 * 10$(pg Cell^{-1} h^{-1}) $\delta = 0.60$, $\alpha = 0.40$, $\kappa = 0.46$(Pa), $n = 1.68$	
12	MMP-1 reduction of collagen to gelatin	25 × MMP1 (pgh^{-1})	Welgus et al. (1980) and Welgus et al. (1981)
13	MMP-2 reduction of gelatin	410 × MMP2 (pg h^{-1})	Xia et al. (1996) and Le et al. (1999)
14	MMP-9 reduction of gelatin	135 × MMP9 (pg h^{-1})	Murphy et al. (1985) and Xia et al. (1996)
15	MMP-2 reduction of elastin	For remaining MMP-2: 2.64 × MMP2 (pg h^{-1})	Murphy et al. (1985), Xia et al. (1996) and Le et al. (1999)
16	MMP-9 reduction of elastin	For remaining MMP-9: 0.87 × MMP9 (pg h^{-1})	Murphy et al. (1985), Xia et al. (1996) and Le et al. (1999)
17	MMP-1 removal	MMP 1/2.8 (pg h^{-1})	MBC
18	MMP-2 removal	MMP2/2.15 (pg h^{-1})	MBC
19	MMP-9 removal	MMP9/2.11 (pg h^{-1})	MBC
20	Fibroblast proliferation chance	a + M(1 − exp(−($PDGF/\kappa$)^n)) (h^{-1}) $a = 1.11e - 3$ (h^{-1}), $M = 9.41e - 3$ (h^{-1}) $\kappa = 0.26$(pg), $n = 1.29$	Kim et al. (1999) and Das et al. (2001)
21	Fibroblast apoptosis chance	0.001112 (h^{-1})	MBC
22	Fibroblast production of collagen (stretch induced)	$b \times (1 + M(\epsilon))$ $M(\epsilon) = 116 * \epsilon^2 + 0.8\epsilon$ $b = 9.23e - 3$ (pg Cell^{-1} h^{-1})	Wu et al. (2014) and Jenkins et al. (2007)
23	Fibroblast production of MMP-1 (constant)	MMP1 = b b = 12.68e−5 (pg Cell^{-1} h^{-1})	Ethier et al. (1982) and Karakiulakis et al. (2007)
24	Fibroblast production of MMP-2 (constant)	MMP2 = b (pg Cell^{-1} h^{-1}) $b = 7.65e$−6 (pg Cell^{-1} h^{-1})	Okuno et al. (2002) MBC
25	Fibroblast production of MMP-9 (constant)	MMP9 = b (pg Cell^{-1} h^{-1}) $b = 0.31e - 6$ (pg Cell^{-1} h^{-1})	Ethier et al. (1982) and Garcia-Lopez et al. (2007) MBC

[a]Mass balance constraint

Author Manuscript

Author Manuscript

Author Manuscript

Author Manuscript

Table 2

Mechanical properties of ECM contents and cells

Content type	Initial shear modulus (kPa)	References
Collagen	442.6	Lu et al. (2004)
Elastin	99	Lu et al. (2004) and Karsaj et al. (2010)
Gelatin	21.9	Norris and McGraw (1964), Lou (1999) and Yakimets et al. (2005)
SMC	4.3	Qiu et al. (2010)
Fibroblast	0.5	Engler et al. (2004)
EC	1.42	Stroka and Aranda-Espinoza (2011)

Author Manuscript

Author Manuscript

Author Manuscript

Author Manuscript

Table 3

Model stability assessed by the average maximal variation of each parameter from its baseline value over 100 days and under either normotensive or normotensive with transient increases in blood pressure condition

Parameter	Normotensive (%)	Transient increases in blood pressure (%)
Collagen	<0.001	<0.001
Elastin	0	0
Gelatin	0	<0.001
SMC	<0.1	<0.01
Fibroblast	0.04	<0.01
EC	0	0
PDGF	<0.001	<0.001
TGF-P	<0.1	<0.001
MMP-1	0.05	<0.001
MMP-2	0.06	<0.001
MMP-9	<0.001	<0.001

Author Manuscript

Author Manuscript

Author Manuscript

Author Manuscript

Table 4

Summary of sensitivity studies of various rule parameters

Rule no.	Description	X10	X0.1
SMCs			
1	Proliferation: M	Unstable	Stable
3	PDGF Production: m	Unstable	Stable
4	TGF-β	Unstable	NS[a]
5	MMP-1	Unstable	Unstable
6	MMP-2: M	Unstable	NS
6	MMP-2: n	Unstable	Unstable
7	MMP-9: M	NS	NS
7	MMP-9: n	NS	NS
8	Collagen: m	NS	NS
Fibroblasts			
20	Proliferation: a	Unstable	Stable
22	Collagen: basal rate	Unstable	NS
22	Collagen: a	Stable	Stable
22	Collagen: b	Stable	Stable
23	MMP-1:b	Unstable	NS
24	MMP-2:b	NS	NS
25	MMP-9:b	NS	NS

[a]Not sensitive